Inositol 1,4,5-Trisphosphate Receptors: Labeling the Inositol 1,4,5-Trisphosphate Binding Site with Photoaffinity Ligands†

Robert J. Mourey,‡ Virginia A. Estevez,§ James F. Marecek,§ Roxanne K. Barrow,‡ Glenn D. Prestwich,§ and Solomon H. Snyder*,‡

Departments of Neuroscience, Pharmacology and Molecular Sciences, and Psychiatry and Behavioral Sciences, Johns Hopkins Medical Institutions, 725 North Wolfe Street, Baltimore, Maryland 21205, and Department of Chemistry, State University of New York at Stony Brook, Stony Brook, New York 11794-3400

Received August 14, 1992; Revised Manuscript Received November 24, 1992

ABSTRACT: We have photolabeled the inositol 1,4,5-trisphosphate (IP_3) receptor and probed the IP_3 ligand binding site using two novel photoaffinity ligands, [^{125}I](azidosalicyl)aminopropyl-IP_3 ([^{125}I]ASA-IP_3) and [^{3}H](benzoyldihydrocinnamyl)aminopropyl-IP_3 ([^{3}H]BZDC-IP_3). Both ligands have high affinity for the IP_3 receptor and, when photoactivated, label the IP_3 receptor protein with appropriate inositol phosphate selectivity. The high specific activity of [^{125}I]ASA-IP_3 allowed identification of a single photolabeling site within the IP_3R by two-dimensional peptide analysis. Substantially higher levels of incorporation into the receptor are achieved with [^{3}H]BZDC-IP_3 (50–60% efficiency) than with [^{125}I]ASA-IP_3 (3%), facilitating the use of [^{3}H]BZDC-IP_3 as a better ligand for the high-efficiency labeling and purification of IP_3R-labeled peptides. Peptides were generated from photolabeled IP_3 receptor by trypsin digestion and purified by high-pressure liquid chromatography (HPLC). A single purified [^{3}H]BZDC-IP_3-labeled peptide, corresponding to IP_3R amino acids 476–501, was sequenced and shown to match specific sequences in the N-terminal 20% of the IP_3 receptor, an area suggested on the basis of mutagenesis studies to contain the IP_3 recognition site.

Inositol 1,4,5-trisphosphate (IP_3),[1] formed by the activation of phospholipase C in response to neurotransmitter or hormone stimulation of receptors, is a prominent intracellular messenger acting through the release of calcium from intracellular stores [for reviews, see Berridge and Irvine (1989), Chuang (1989), Fischer et al. (1992), and Ferris and Snyder (1992)]. IP_3 binds to its receptor, a protein largely associated with subcompartments of the endoplasmic reticulum (Ross et al., 1989; Otsu et al., 1990; Satoh et al., 1990), but in some instances possibly associated with the plasma membrane (Kuno & Gardner, 1987; Ronnett & Snyder, 1992). The IP_3 receptor (IP_3R) has been purified from rat brain (Supattapone et al., 1988) and shown by reconstitution experiments to contain both the IP_3 recognition site and an associated calcium channel (Ferris et al., 1990).

IP_3R cDNAs have been cloned from mouse (Furuichi et al., 1989), rat (Mignery et al., 1990), and human (Ross et al., 1991). Hydrophobicity analysis indicates that the IP_3R contains eight transmembrane regions at the extreme carboxyl-terminal 600 amino acids, which likely constitute the calcium channel (Mignery et al., 1990). The great majority of the 2749 amino acid IP_3R protein is cytoplasmic, consisting of both an IP_3 binding domain in the amino-terminal fourth of the receptor (Mignery et al., 1990) and a large putative "coupling domain" of over 1400 amino acids. The large molecular distance between the IP_3 binding domain and the putative calcium channel implies conformational change upon IP_3 binding, as has been observed by Mignery and Südhof (1990). The coupling domain, containing two putative ATP binding sites (Ferris & Snyder, 1992), alternative splicing sites (Danoff et al., 1991; Nakagawa et al., 1991), and two identified phosphorylation sites for cAMP-dependent protein kinase (Ferris et al., 1991), may also be involved in IP_3R channel regulation.

In efforts to identify the IP_3R domain containing the IP_3 recognition site, Mignery and Südhof (1990) utilized mutagenesis to construct truncated IP_3R molecules, progressively removing larger portions of the C-terminal region. IP_3 binding was retained in truncated receptors comprising only the N-terminal 788 amino acids, while a mutant comprised of the N-terminal 519 amino acids failed to display IP_3 binding, indicating that IP_3 binds within the N-terminal 788 amino acids of the IP_3R. In a more detailed deletion mutagenesis study, Miyawaki et al. (1991) constructed mutants deleting a few hundred amino acids from different portions of the IP_3R and observed loss of IP_3 binding in four mutants with deletions within the N-terminal 735 amino acids.

To further define the IP_3 recognition site, we have radiolabeled IP_3R using photoaffinity derivatives of IP_3. We now report the selective labeling of one peptide, which we have sequenced and shown to occur in the extreme N-terminal portion of IP_3R.

† Supported by USPHS Grants MH-18501, Research Scientist Award DA-00074 to S.H.S., Training Grant GM-07626 to R.J.M., a gift from Bristol-Myers Squibb, a W. Burghardt Turner Fellowship to V.A.E., and a grant from the Center for Biotechnology and the New York State Foundation for Science and Technology to G.D.P. and J.F.M.

* To whom correspondence and reprint requests should be addressed at the Department of Neuroscience, Johns Hopkins Medical Institutions, 725 N. Wolfe St., Baltimore, MD 21205-2185; tel (410) 955-3024, fax (410) 955-3623.

‡ Johns Hopkins Medical Institutions.

§ State University of New York at Stony Brook.

[1] Abbreviations: Ins, *myo*-inositol; IP_1, inositol 1-monophosphate; IP_2, inositol 1,4-bisphosphate; IP_3, inositol 1,4,5-trisphosphate; IP_4, inositol 1,3,4,5-tetrakisphosphate; IP_5, inositol 1,3,4,5,6-pentakisphosphate; IP_6, inositol 1,2,3,4,5,6-hexakisphosphate; IP_3R, IP_3 receptor; [^{125}I]ASA-IP_3, [^{125}I]-1-*O*-[*N*-(4-azidosalicyl)-3-aminopropyl-1-phospho]-*myo*-inositol 4,5-bisphosphate; [^{3}H]BZDC-IP_3, [^{3}H]-1-*O*-[*N*-(benzoyldihydrocinnamyl)-3-aminopropyl-1-phospho]-*myo*-inositol 4,5-bisphosphate; CHAPS, 3-[(3-cholamidopropyl)dimethylammonio]-1-propanesulfonate; Con A, concanavalin A; SDS–PAGE, sodium dodecyl sulfate–polyacrylamide gel electrophoresis; TFA, trifluoroacetic acid; HPLC, high-pressure liquid chromatography.

0006-2960/93/0432-1719$04.00/0

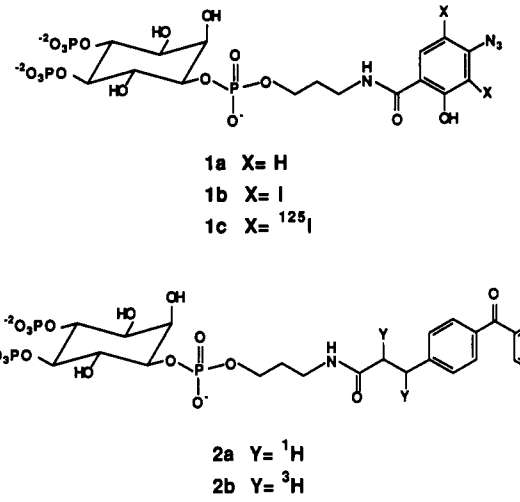

FIGURE 1: IP_3 photoaffinity ligands. Photoaffinity ligands **1a**, **1b**, **1c**, **2a**, and **2b** were synthesized as described in Materials and Methods.

MATERIALS AND METHODS

Materials. All reagents and solvents for photoaffinity ligand synthesis were purchased from either Aldrich Chemical Co. or Fischer Scientific and were of reagent grade. Reverse-phase HPLC was performed on a Brownlee RP-300 C_8 column (0.45 cm × 22 cm) using an LKB gradient system equipped with an LKB 2140 diode array detector and an IN/US β-RAM online radioactivity detector. Hydrogenation with carrier-free tritium gas was carried out at NEN/DuPont Laboratories. [^{3}H]Inositol 1,4,5-trisphosphate ([^{3}H]IP_3, 20 Ci/mmol), ENHANCE, and PROTOSOL were from NEN/DuPont (Boston, MA). Unlabeled inositol phosphates were from Calbiochem (La Jolla, CA) and nitrocellulose was purchased from Schleicher & Schuell (Keene, NH). Trypsin, thermolysin, and endoproteinase Glu-C were obtained from Boehringer Mannheim (Indianapolis, IN). HPLC gel filtration standards were purchased from Gibco BRL (Gaithersburg, MD). Protein concentration was determined using Coomassie Protein Assay Reagent from Pierce (Rockford, IL). All other reagents were obtained from Sigma (St. Louis, MO).

Synthesis of Photoaffinity Ligands (Figures 1 and 2). (*A*) *(Azidosalicyl)aminopropyl-IP$_3$* (**1a–c**). The synthesis of both [^{125}I]-labeled and unlabeled azidosalicylamide derivatives of IP_3 has been previously described (Prestwich et al., 1991; Kalinoski et al., 1992). The specific activity of **1c** was 800 Ci/mmol.

(*B*) *α-Bromo-p-benzoylhydrocinnamic Acid* (**3**). *p*-Aminobenzophenone [1.80 g (9.13 mmol)] was treated with 2.7 mL of concentrated HBr followed by 15 mL of acetone. After stirring for 15 min, the reaction was cooled to 4 °C and diazotized with 0.5 M $NaNO_2$. The brown solution was maintained at 4 °C and stirred for 3 min. Freshly distilled acrylic acid (8.8 mL, 0.13 mol) was then added and the mixture vigorously stirred under a heavy flow of argon. After 15 min, 25 mg of cuprous bromide (CuBr) was added. Nitrogen was evolved immediately after the addition of CuBr, and the mixture was stirred for 30 min during which time it was allowed to warm to room temperature. The reaction was poured into 200 mL of water and an orange oil separated. The oil was pipetted out from the water layer, diluted with 25 mL of $CHCl_3$, washed with water (2 × 25 mL), dried over $MgSO_4$, filtered, and concentrated in vacuo. The resultant oil was chromatographed on silica gel ($CHCl_3$) to provide 2.76 g (91%) of the acid **3** as a yellow oil. ^{1}H NMR (300 MHz, $CDCl_3$) δ 3.33 (dd, 1 H, J = 7.8 and 14.4 Hz, 3.56 (dd, 1 H, J = 7.5 and 14.1 Hz), 4.84 (t, 1 H, J = 10.2 Hz), 7.36 (d, 2 H, J = 8.1 Hz), 7.48 (t, 2 H, J = 8.4 Hz), 7.60 (t, 1 H, J = 7.5 Hz), 7.78 (m, 4 H), 9.45 (bs, 1 H); ^{13}C NMR (75 MHz, $CDCl_3$) δ 40.68, 44.13, 128.9, 129.1, 130.0, 130.5, 132.48, 136.73, 137.52, 141.26, 173.3, 196.5.

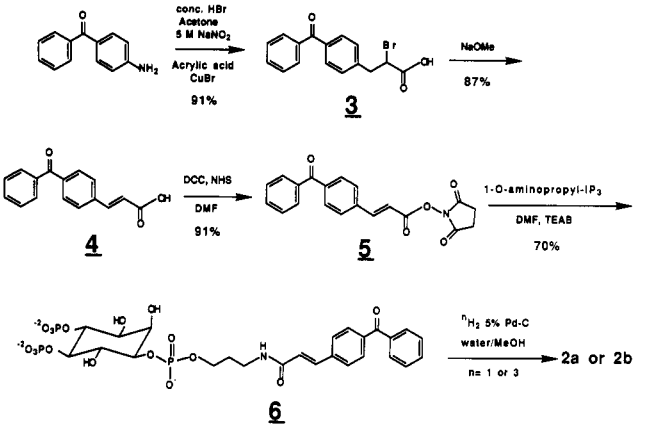

FIGURE 2: Synthesis of BZDC-IP_3. BZDC-IP_3 and [^{3}H]BZDC-IP_3 (**2a** and **2b**) were synthesized as described in Materials and Methods. Reaction step yields are shown as percentages.

(*C*) *p-Benzoylcinnamic Acid* (**4**). A suspension of 1.83 g (5.49 mmol) of α-bromo-*p*-benzoylhydrocinnamic acid (**3**) in 40 mL of MeOH and 5.00 g of NaOH was stirred at room temperature. Immediately, the yellow color of the solution disappeared and a chalky off-white precipitate formed. After stirring for 5 min, the suspension was concentrated in vacuo. The resulting wet solid was dissolved in 125 mL of water and then acidified with concentrated hydrobromic acid, forming a white precipitate. The suspension was kept in the refrigerator overnight to induce more precipitation. The solid was isolated by filtration and washed with water to give 1.21 g (87%) of **4** as a white solid. ^{1}H NMR (300 MHz, DMSO-d_6 δ 5.44 (d, 1 H, J = 15.9 Hz), 6.33 (t, 2 H, J = 7.5 Hz), 6.43 (d, 1 H, J = 15.6 Hz), 6.49–6.55 (m, 5 H), 6.62 (d, 2 H, J = 8.4 Hz); ^{13}C NMR (75 MHz, DMSO-d_6) δ 122.2, 128.5, 129.0, 129.9, 130.4, 133.1, 137.3, 138.4, 138.6, 142.9, 176.6, 195.7.

(*D*) *N-Succinimidyl p-Benzoylcinnamate* (**5**). To a solution of 515 mg (2.04 mmol) of *p*-benzoylcinnamic acid (**4**) in 12 mL of dimethylformamide (DMF) at room temperature was added 235 mg (2.04 mmol) of *N*-hydroxysuccinimide. After 3 min of stirring, a solution of 421 mg (2.04 mmol) of dicyclohexylcarbodiimide (DCC) in 3 mL of DMF was added. A white precipitate formed after 1 h of stirring. The reaction was stirred overnight, cooled in an ice bath, and filtered. The filtrate was concentrated in vacuo and triturated with CH_2Cl_2. The precipitate formed was removed by filtration and the filtrate treated with ethyl ether/petroleum ether to give after filtration 649 mg (91%) of the *N*-hydroxysuccinimidyl ester **5** as white crystals. ^{1}H NMR (300 MHz, $CDCl_3$) δ 2.90, (d, 1 H, J = 15.9 Hz), 7.51 (t, 2 H, J = 7.8 Hz), 7.62 (tt, 1 H, J = 1.7 and 6.4 Hz), 7.69 (d, 2 H, J = 8.1 Hz), 7.83 (m, 4 H), 7.97 (d, 1 H, J = 15.9 Hz); ^{13}C NMR (75 MHz, $CDCl_3$) δ 25.61, 113.92, 128.39, 128.42, 129.99, 130.6, 132.6, 137.0, 137.2, 148.4, 161.6, 169.2, 195.9.

(*E*) *(p-Benzoylcinnamyl)aminopropyl-IP$_3$* (**6**). To a solution of 42.9 mg (0.0779 mmol) of 1-*O*-(3-aminopropyl-1-phospho)-*myo*-inositol 4,5-bisphosphate in 1.8 mL of 0.25 M aqueous triethylammonium bicarbonate (TEAB), pH 8.5, was added a solution of 81.6 mg (0.234 mmol) of *N*-succinimidyl *p*-benzoylcinnamate (**5**) in 4.5 mL of DMF at room temperature. A white precipitate formed immediately. After stirring overnight, the suspension was concentrated in vacuo,

suspended in 10 mL of water, centrifuged, decanted, and concentrated in vacuo. The white residue was redissolved in 3 mL of water and applied to a column of DEAE-cellulose (HCO_3^- form). The column was washed with 25 mL of water and eluted with 15 mL of 0.1 M TEAB, 30 mL of 0.2 M TEAB, 15 mL of 0.3 M TEAB, 15 mL of 0.4 M TEAB, and 15 mL of 0.6 M TEAB. Analysis of the fractions by reverse-phase HPLC (15% acetonitrile in 0.05 M KH_2PO_4 buffer, pH 4.5) showed a single product in the 0.3 and 0.4 M TEAB eluate fractions with a retention time of 18 min (UV_{max} at 300 nm). The fractions containing the desired product were combined, concentrated in vacuo, applied to a Chelex column (Na^+ form), and eluted with 40 mL of water. The eluate was concentrated in vacuo to give 43 mg (70%) of **6** as a colorless solid. ^1H NMR (300 MHz, D_2O) δ 1.74 (m, 2 H), 3.23 (t, 2 H, J = 6.3 Hz), 3.58 (dd, 1 H, J = 2.5 Hz), 3.72–4.11 (m, 5 H); ^{13}C NMR (75 MHz, D_2O) δ 30.11 (d, J = 5.6 Hz), 37.07, 64.29 (d, J = 5.5 Hz), 71.22, 72.39 (apparent t, J = 5.9 Hz), 75.17 (apparent t, J = 5.4 Hz), 76.71 (d, J = 4.6 Hz), 77.32, 123.9, 127.9, 128.2, 129.1, 130.5, 131.12, 133.93, 137.2, 139.6, 168.44, 199.9.

(F) (Benzoyldihydrocinnamyl)aminopropyl-IP₃ (**2a,b**). To a solution of 16 mg of (*p*-benzoylcinnamyl)aminopropyl-IP_3 (**6**) in 2.0 mL of water and 0.5 mL of ethanol was added 8.5 mg of 5% Pd–C. The reaction mixture was stirred under 1 atm of hydrogen gas at room temperature for 2 h. The reaction was followed by reverse-phase HPLC (as above) and showed one product with a retention time of 11 min and a UV_{max} at 286 nm. The reaction mixture was then concentrated in vacuo and the residue applied to a column packed with DEAE-cellulose (HCO_3^-). The column was washed with 10 mL of water and eluted with 5-mL aliquots of 0.2, 0.3, 0.4, and 0.6 M TEAB. Analysis of the fractions by reverse-phase HPLC showed a single product in the 0.3 and 0.4 M TEAB eluate fractions. These fractions were combined, concentrated in vacuo, applied to a Chelex column (Na^+ form), and eluted with water. The eluate was concentrated in vacuo to give 1.3 mg of **2a** as a white solid. ^1H NMR (300 MHz, D_2O) δ 1.52 (q, 2 H, J = 6.5 Hz), 2.44 (t, 2 H, J = 7.5 Hz), 2.89 (t, 2 H, J = 7.5 Hz), 3.06 (t, 2 H, J = 6.5 Hz), 3.39–4.8 (m, 8 H), 7.27 (d, 2 H, J = 8.1 Hz), 7.44 (t, 2 H, J = 7.5 Hz), 7.56–7.68 (m, 5 H).

Hydrogenation of **6** with carrier-free tritium gas was performed by NEN/DuPont under identical conditions as for the synthesis of **2a**. Purification of **2b** was carried out using a Waters C_{18} Sep-Pak. The cartridge was washed with 50 nM phosphate buffer (pH 4.5) and eluted with 5%, 10%, 15%, and 20% acetonitrile in phosphate buffer. The desired product **2b** eluted in the 15–20% acetonitrile fractions with a specific activity of approximately 4 Ci/mmol.

Photoaffinity Ligand Binding to IP_3R. Washed rat cerebellar membranes, 1% CHAPS detergent-solubilized membranes, heparin column eluate, and concanavalin A (Con A) column eluate purification fractions were prepared (Supattapone et al., 1988; Mourey et al., 1990), and photoaffinity ligand binding was conducted as follows. Binding with [^{125}I]-ASA-IP_3 and [^{3}H]BZDC-IP_3 photoaffinity ligands, respectively, employed dark and subdued lighting conditions. Binding to membrane fractions used 100 μL of washed membranes, 4 nM [^{125}I]ASA-IP_3 or 10 nM [^{3}H]BZDC-IP_3, and buffer (50 mM Tris, pH 8.4/2 mM EDTA/1 mM 2-mercaptoethanol) in a total volume of 0.5 mL. Binding assays with detergent-solubilized IP_3R fractions were as described above with the exception of using 200-μL sample fractions with buffer containing 1% CHAPS. Reactions at 0 °C were allowed to reach equilibrium at 10 min and then photoactivated as described below. Following photolabeling, Laemmli sample buffer (5×) was added to the samples and photolabeled IP_3R separated on 1.5 mm thick 7.5% SDS–PAGE gels (Laemmli, 1970). Protein was stained with Coomassie Blue, and the gels were dried at 65 °C in vacuo. [^{125}I]ASA-IP_3-labeled IP_3R gels were subjected to autoradiography (48 h, –70 °C), or the stained IP_3R band was cut out and radioactivity determined directly. Either [^{3}H]BZDC-IP_3-labeled IP_3R gels were treated for fluorography using ENHANCE and subjected to autoradiography (10 days, –70 °C), or the stained IP_3R bands were excised, with radioactivity extracted by incubation at 37 °C overnight with 2 mL of PROTOSOL and counted by liquid scintillation chromatography. Specific binding represented less than 10% of added ligand. Nonspecific binding was determined in the presence of 10 μM unlabeled IP_3.

Photoactivation of IP_3 Photoaffinity Ligands. [^{125}I]ASA-IP_3-incubated samples were photolabeled when exposed in quartz test tubes to 4 × 30 s of short-wave (254-nm) UV radiation at a distance of 1.5 cm with 20 s of cooling (0 °C) in the dark between exposures. [^{3}H]BZDC-IP_3-incubated samples were photolabeled for 35 min using a polystyrene tissue culture dish (35 × 10 mm) on ice placed 5 cm from a 100-W long-wave (365-nm) BlakRay UV lamp (UVP, Inc).

Peptide Purification. Purified IP_3R from the Con A column eluate fraction (Supattapone et al., 1988; Mourey et al., 1990) was diluted 20-fold with 50 mM Tris, pH 8.4/2 mM EDTA/1 mM 2-mercaptoethanol/1% CHAPS buffer (buffer A) and concentrated with Centriprep 30 (Amicon) ultrafiltration concentrators. To generate large amounts of photolabeled IP_3R peptide for purification and sequencing, binding reactions consisted of 1 mg of purified IP_3R (approximately 4 nmol), 1 μM [^{3}H]BZDC-IP_3 (10 μCi), 4 μM unlabeled BZDC-IP_3, and buffer A to a volume of 2.5 mL. Binding conditions and photolabeling were as described above. Laemmli sample buffer (5×) was added to terminate the reaction and the IP_3R protein resolved on two preparative 3-mm 7.5% SDS–PAGE gels. Following SDS–PAGE, proteins were transferred to nitrocellulose (24 h, 200 mA, 4 °C) in transfer buffer (20 mM Tris base/150 mM glycine/20% methanol) and visualized with Ponceau-S stain. The 260-kDa IP_3R protein bands were cut out of the blot, denatured, reduced, and alkylated and the membranes blocked as described (Ferris et al., 1991). The blot pieces were finely diced, and the protein was digested to completion with 50 μg of trypsin for 20 h at 37 °C in 50 mM NH_4HCO_3, pH 7.8, buffer (Ferris et al., 1991). Following digestion, over 90% of the radioactivity was recovered in the supernatant, and the peptides were lyophilized to dryness and resuspended in water for injection onto HPLC (Hewlett-Packard HP 1090 liquid chromatograph).

Trypsin fragments were injected onto a C_8 reverse-phase column (Aquapore RP-300/micron, 220 × 2.1 mm), washed for 10 min with 0.06% trifluoroacetic acid (TFA), and eluted with a 140-min 0–80% acetonitrile/0.06% TFA gradient at a 0.3 mL/min flow rate. Eluting peptides were monitored at an absorbance of 214 nm and the peaks collected by hand into polypropylene microcentrifuge tubes. Peptide peaks containing radioactivity were lyophilized to near dryness, injected onto a second HPLC reverse-phase column (Vydac, 219TP52 phenyl, 2.1 × 250 mm), and eluted at 0.2 mL/min as described above. In all cases, a single peptide peak containing greater than 90% of radioactivity was obtained and its sequence determined by Edman degradation (Applied Biosystems Automated Sequencer).

Table I: Affinity of IP_3 Photoaffinity Analogues for the IP_3 Receptor[a]

compound	K_i (nM)
IP_3	10
1a	236
1b	80
2a	500

[a] K_i values were determined by competition of compounds with [^{3}H]IP_3 binding to washed rat cerebellar membranes (Supattapone et al., 1988). Data are mean values of experiments conducted twice in triplicate.

RESULTS

Photoaffinity Labeling of IP_3 Receptors with [^{125}I]ASA-IP_3 and [^{3}H]BZDC-IP_3. Previously we demonstrated that IP_4 and IP_6 receptor binding sites can be selectively labeled with a photoaffinity ligand bearing an azidosalicylyl moiety linked to IP_4 by an aminopropyl tether at the 1-phosphate position (Theibert et al., 1992). Using a similar synthetic strategy, the (azidosalicyl)aminopropyl-IP_3 derivative (Figure 1, compound **1a**) was generated and shown to bind reversibly with high affinity to IP_3R, with 20-fold less affinity than IP_3 (Prestwich et al., 1991). Interestingly, the iodination of ASA-IP_3 (Figure 1, compound **1b**) leads to a 3-fold increase in affinity for the IP_3R (Table I) and 8-fold less affinity than IP_3, suggesting that the more lipophilic photoreactive group may interact more favorably with a hydrophobic region proximal to the IP_3 binding site.

A second IP_3 photoaffinity ligand was developed utilizing the same aminopropyl tether linkage to IP_3 but conjugated to a benzoylcinnamic acid photoreactive moiety via the propylamine (Figure 2, compound **6**). The benzoylphenyl photophore was selected because of its reported higher efficiency of bimolecular photoattachment, i.e., up to 70% in several cases involving *p*-benzoylphenylalanine-containing peptides (Kauer et al., 1986; Miller & Kaiser, 1988; Boyd et al., 1991). This unsaturated IP_3 photoaffinity ligand can be reductively tritiated to generate [^{3}H](benzoyldihydrocinnamoyl)aminopropyl-IP_3 (Figure 1, compound **2b**). In reversible [^{3}H]IP_3 binding experiments to rat cerebellar membranes, unlabeled BZDC-IP_3 (Figure 1, compound **2a**) has a 50-fold lower affinity than IP_3 (Table I), possibly due to steric hindrance from the large photoreactive group. The actual affinity of BZDC-IP_3 for the IP_3 receptor may be greater, however, due to the increased hydrophobicity of this ligand, which may lead to partitioning and an underestimation of the actual free ligand concentration.

In the present study, we confirm the high affinity and selective reversible binding of [^{125}I]ASA-IP_3 to both crude and purified IP_3R (data not shown). Following photoactivation with short-wave UV irradiation, in rat cerebellar membranes we observe the incorporation of [^{125}I]ASA-IP_3 into a 260-kDa protein (Figure 3A), corresponding to IP_3R detected by immunoreactivity in parallel experiments by Western blot analysis (data not shown). Specificity of photolabeling is evident by the total absence of labeling of the 260-kDa protein conducted in the presence of 10 μM IP_3. One other prominently labeled protein at approximately 28 kDa represents nonspecific labeling, as it is not displaced by unlabeled IP_3. In crude detergent-solubilized membranes a larger number of proteins are labeled, presumably due to the greater exposure of proteins to the photoligand reactive group, although only the 260-kDa protein is displaced by unlabeled IP_3. In eluates of the heparin column, labeling of the IP_3R protein is most prominent and displaceable, while in the completely purified receptor (Con A eluate) only a single protein is evident.

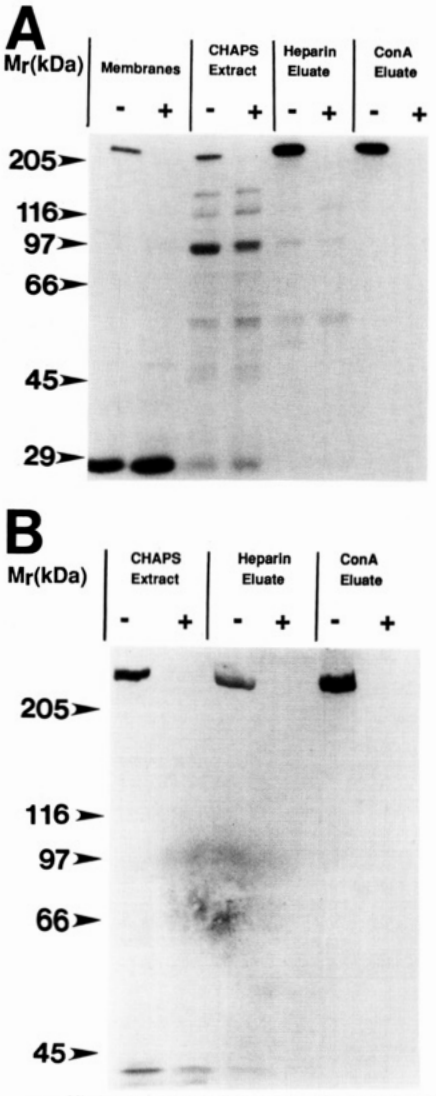

FIGURE 3: Photoaffinity labeling of fractions during the purification of IP_3R. Washed cerebellar membranes, CHAPS-solubilized membranes (CHAPS extract), heparin eluate, and Con A eluate fractions were prepared, photolabeled with (A) [^{125}I]ASA-IP_3 and (B) [^{3}H]-BZDC-IP_3, and subjected to SDS–PAGE as described in Materials and Methods. Photolysis reaction times for [^{125}I]ASA-IP_3 and [^{3}H]-BZDC-IP_3 were 30 s and 35 min, respectively. Specificity of photolabeling was determined in the absence (–) or presence (+) of 10 μM unlabeled IP_3. Autoradiograms of a typical purification scheme that was repeated three times with similar results are shown. No photolabeling was detected in the membrane fraction photolabeled with [^{3}H]BZDC-IP_3.

To ascertain the inositol phosphate specificity of photolabeling, we conducted photolabeling with [^{125}I]ASA-IP_3 in the presence of various concentrations of inositol phosphates (Figure 4A). The photoaffinity labeling is highly selective, with IP_3 being most potent, providing 50% displacement at approximately 100 nM. IP_4 displays an IC_{50} of 2 μM, with the other inositol phosphates being substantially less potent. These relative potencies correspond to the known inositol phosphate specificity of IP_3R (Supattapone et al., 1988), ensuring that photolabeling is selective. Similar inositol phosphate potencies and specificities are observed with reversible [^{125}I]ASA-IP_3 binding to cerebellar membranes (data not shown).

Photolabeling with [^{125}I]ASA-IP_3 at 254 nm is extremely rapid. At the earliest time point examined, approximately 30 s, maximal levels of specific binding are apparent with total binding 10 times greater than nonspecific binding monitored in the presence of 10 μM IP_3 (data not shown). In contrast

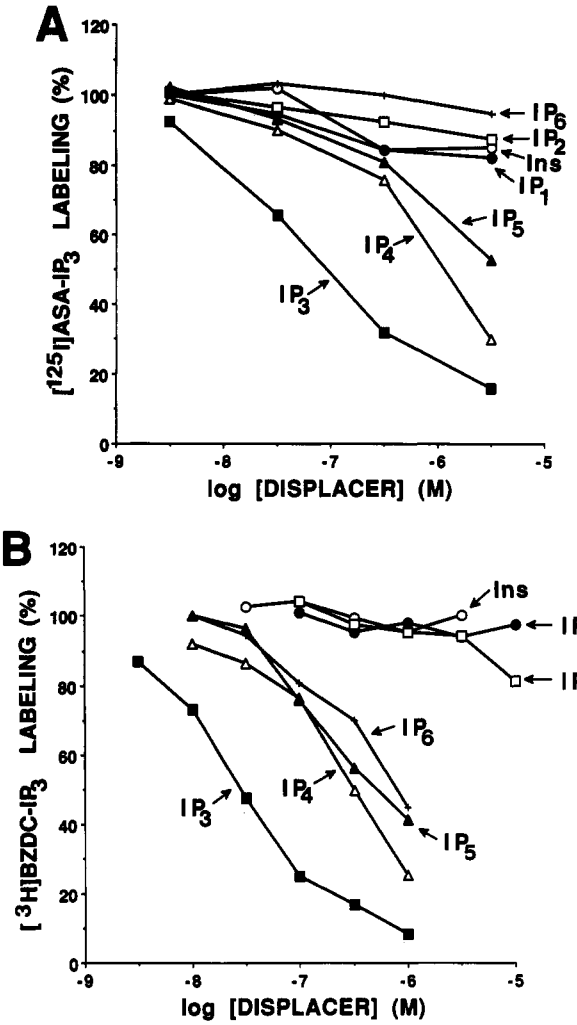

FIGURE 4: Inositol phosphate specificity of IP_3R photolabeling. Photolabeling of the IP_3R (heparin eluate fraction) with (A) [^{125}I]-ASA-IP_3 and (B) [^{3}H]BZDC-IP_3 was conducted as described in Materials and Methods. Photolysis reaction times for [^{125}I]ASA-IP_3 and [^{3}H]BZDC-IP_3 were 30 s and 35 min, respectively. Inositol phosphates evaluated were *myo*-inositol (Ins), 1-IP_1, 1,4-IP_2, 1,4,5-IP_3, 1,3,4,5-IP_4, 1,3,4,5,6-IP_5, and 1,2,3,4,5,6-IP_6. Results, expressed as percent inhibition of maximal specific labeling, are from a typical experiment repeated three times in duplicate.

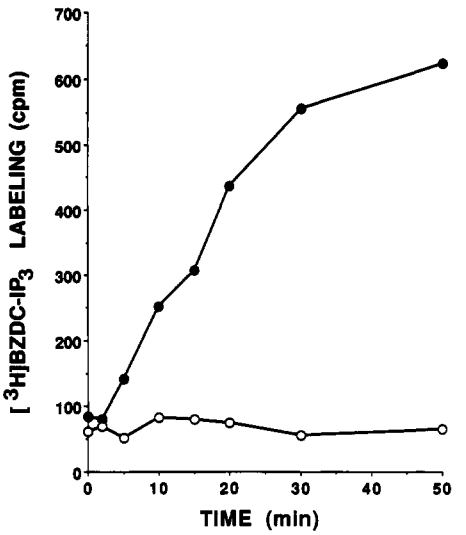

FIGURE 5: Time course of IP_3R photolabeling with [^{3}H]BZDC-IP_3. Purified IP_3R was photolabeled for various times in the absence (closed circles) or presence (open circles) of 10 μM unlabeled IP_3, and the detection of incorporated [^{3}H]BZDC-IP_3 radioactivity was as described in Materials and Methods. Data shown are from a typical experiment repeated twice in duplicate with essentially the same results.

to the rapid photolabeling with [^{125}I]ASA-IP_3, the photoactivation of [^{3}H]BZDC-IP_3 occurs much more slowly (Figure 5), as expected for the lower molar absorptivity of the benzophenone chromaphore at 360 nm. Maximal photolabeling occurs between 30 and 40 min, with total covalent labeling approximately 6–7 times nonspecific levels in the presence of 10 μM unlabeled IP_3. Half-maximal labeling is evident at about 15 min.

As with [^{125}I]ASA-IP_3, [^{3}H]BZDC-IP_3 photolabeling is highly selective, labeling only a single 260-kDa protein in the crude detergent-solubilized fraction as well as the heparin eluate and Con A-purified IP_3R fractions (Figure 3B). Interestingly, in contrast to [^{125}I]ASA-IP_3 photolabeling, [^{3}H]-BZDC-IP_3 labels fewer nonspecific proteins. Only two lightly labeled proteins of approximately 40 and 37 kDa are evident in the crude detergent extract with no other nonspecific labeled proteins observed. No photolabeling is detected in the crude membrane fraction (data not shown), possibly due to the inability of the longer wave ultraviolet radiation to penetrate the opaque membrane suspension.

Photoaffinity labeling with [^{3}H]BZDC-IP_3 displays considerable inositol phosphate specificity (Figure 4B). IP_3 is most potent, with an IC_{50} of 30 nM, while IP_4, IP_5, and IP_6 are less potent, with similar IC_{50} values of 0.5–1 μM. Inositol, IP_1, and IP_2 do not compete for [^{3}H]BZDC-IP_3 labeling. Similar inositol phosphate specificities and potencies are detected with reversible [^{3}H]BZDC-IP_3 binding to cerebellar membranes (data not shown).

The number of sites labeled within the IP_3R by [^{125}I]ASA-IP_3 was analyzed by two-dimensional peptide analysis (Figure 6). In all cases, digestion of labeled IP_3R with trypsin, thermolysin, cyanogen bromide, and endoproteinase Glu-C generates one labeled peptide spot. Although several of the labeled peptides chromatograph similarly, their migrations are not identical. The radiolabeled peptides appear to be highly acidic, reflecting either the acidic contribution from the covalently-attached photoaffinity ligand or acidic properties of the constituent amino acids. It is unlikely that SDS bound to the peptides contributes to the overall acidic charge since most of the SDS is removed during urea extraction of the IP_3R. Also, under similar peptide generating conditions, the phosphorylated IP_3R yields basic peptides (Ferris et al., 1991). The generation of a single radioactive peptide, rather than multiple labeled peptides, contributes to the degree of specificity of [^{125}I]ASA-IP_3 as a photoaffinity ligand for the IP_3R. Attempts to generate analogous peptide maps of [^{3}H]-BZDC-IP_3-photolabeled IP_3R were unsuccessful, possibly due to the low specific activity of the photoaffinity ligand relative to the higher energy, higher specific activity [^{125}I]ASA-IP_3 ligand.

Purification and Sequencing of IP_3R Peptides Labeled by [^{3}H]BZDC-IP_3. To determine the feasibility of purifying and sequencing IP_3R peptides, we photoaffinity labeled IP_3R with [^{125}I]ASA-IP_3 and [^{3}H]BZDC-IP_3 and monitored incorporated radioactivity (data not shown). Using [^{125}I]ASA-IP_3, only approximately 3% of the IP_3R is labeled, while with [^{3}H]-BZDC-IP_3 the efficiency of photochemically-induced incorporation is dramatically higher, approximately 50%. In initial experiments with [^{125}I]ASA-IP_3-photolabeled IP_3R, attempts to purify peptides (as described in Materials and Methods) were unsuccessful, as quantities of labeled peptide obtained were insufficient for sequencing. This presumably derives

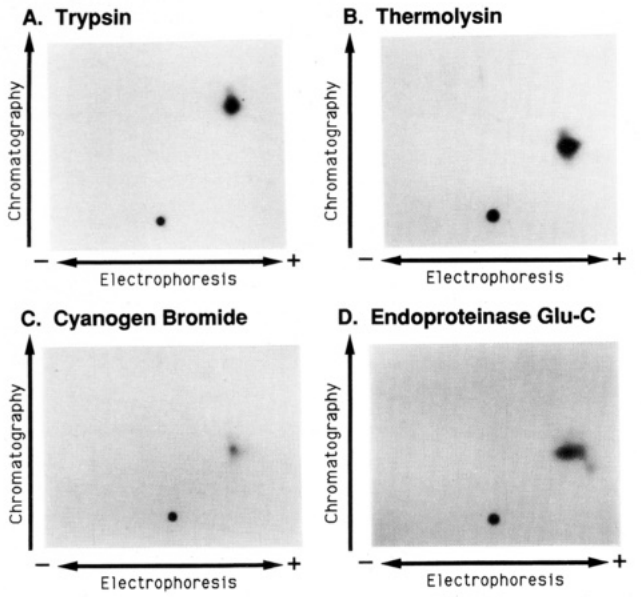

FIGURE 6: Two-dimensional peptide map of [^{125}I]ASA-IP$_3$-photolabeled IP$_3$R. Purified IP$_3$R was photolabeled and subjected to SDS–PAGE as described in Materials and Methods. After SDS–PAGE, the IP$_3$R bands were cut out of the gel and digested by incubating the gel slices in 50 mM NH_4HCO_3, pH 7.8, for 20 h with 30 μg/mL trypsin, thermolysin, or endoproteinase Glu-C at 37, 30, and 25 °C, respectively. For cyanogen bromide digestion, 50 mg/mL in 70% formic acid was used. Following digestion, the peptides were lyophilized, spotted on 20- × 20-cm cellulose thin-layer chromatography plates, and separated by electrophoresis and chromatography as described (Huganir et al., 1984). Electrophoresis was carried out in one dimension at 500 V for 40 min in pyridine/acetic acid/water, 1:10:89 (v/v), pH 3.5. The plates were dried and subjected to ascending chromatography in the second dimension for 3 h in pyridine/butanol/acetic acid/H_2O, 15:10:3:12 (v/v). The plates were then dried and autoradiographed. Shown are autoradiograms (24-h exposure at −70 °C) from an experiment that was repeated twice with similar results. Closed circles represent the origin.

from the low efficiency (3%) of [^{125}I]ASA-IP$_3$ incorporation into the IP$_3$R as well as from photodeiodination of radioiodinated aryl azides (Watt et al., 1989).

We have obtained substantially greater success in purifying and sequencing IP$_3$R peptides photoaffinity labeled with [^{3}H]-BZDC-IP$_3$ (as described in Materials and Methods). The photolabeled IP$_3$R (Con A eluate) was further purified by SDS–PAGE, transferred to nitrocellulose, reduced, and alkylated to prevent renaturation. Following treatment with trypsin, the eluted peptides were fractionated on a C_8 reverse-phase HPLC column (Figure 7A). The C_8 column chromatogram reveals a single main peak of radioactivity eluting at approximately 45 min containing 40% of the total radioactivity eluting from the C_8 column. Broad and diffuse peaks of radioactivity precede and follow the major radioactive peak and may represent nonspecifically labeled peptides. Higher levels of nonspecific labeling than in Figure 5 would be expected due to the increased amounts of radioactive photoaffinity ligand used for preparative labeling. A parallel experiment using 50 μM unlabeled BZDC-IP$_3$ decreases the 45-min eluting radioactive peak greater than 70% while not significantly reducing other radioactive peaks (data not shown). Fractions with high levels of radioactivity were pooled, pool A (25–39 min), pool B (40–50 min), and pool C (51–75 min), and rechromatographed by phenyl reverse-phase HPLC. We were unable to obtain sufficient quantities of purified radiolabeled peptides from pools A and C for sequence determination analysis.

The phenyl column chromatogram of pool B (Figure 7B) reveals a single peak of radioactivity corresponding to an elution time of 44 min, with two broad peaks of low-level radioactivity eluting later. Sequencing of the purified radiolabeled peptide, estimated to be 80% pure, reveals 6 amino acids, LLEDLV, at which point sequencing abruptly stops (Table II). These amino acids correspond to the six amino acids commencing with position 476 of rat IP$_3$R (Table II). Based on known trypsin cleavage sites, the predicted size of the purified peptide should be 26 amino acids. The abrupt cessation of sequencing of the peptide after valine may indicate that the photoaffinity ligand incorporated into the peptide backbone between valine-481 and tyrosine-482. Such an abrupt termination of peptide sequencing was also observed with a similar benzophenone-derived photoaffinity ligand used to label the cAMP-dependent protein kinase substrate binding site (Miller & Kaiser, 1988). We cannot rule out the possibility that the recovery of sequenced amino acids dropped below the level of detection, although the Edman degradation sequencing reaction is routinely sensitive to low picomole quantities.

DISCUSSION

In the present study we have selectively labeled IP$_3$R with two photoaffinity ligands. The ASA group (Ji et al., 1985) of [^{125}I]ASA-IP$_3$ provides rapid and specific incorporation of label into the receptor with readily detectable amounts of radioactivity contributed by the high energy of the ^{125}I radioisotope. Unfortunately, the efficiency of photoinduced covalent attachment to protein relative to rearrangement of the long-lifetime aryl azide-derived nitrenes is particularly low (Leyva et al., 1989). Moreover, the low efficiency is compounded by loss of radiolabel due to photodeiodination occurring in competition with photolabeling (Watt et al., 1989). Nonetheless, our results with the aminopropyl-tethered [^{125}I]-ASA-IP$_3$ clearly indicate that both the selection of the P-1 position and the aminopropyl tether allow specific active-site modification of the 260-kDa IP$_3$R. Less satisfactory results were obtained using a P-1 aminoethyl-tethered [^{125}]ASA-IP$_3$ ligand (Schäfer et al., 1990) which was reported to label three smaller proteins (49, 37, and 31 kDa). Thus, we were unable to obtain amino acid sequence from the small amounts of isolated [^{125}I]ASA-IP$_3$-labeled peptide. Had radiolabeled peptides comigrated with the unlabeled peptides, presumably there would have been enough peptide to sequence. This presumption is based on the previous success of our laboratory in purifying and sequencing IP$_3$R peptides for the identification of cAMP-dependent protein kinase phosphorylation sites (Ferris et al., 1991). Since recoveries of [^{125}I]ASA-IP$_3$-labeled peptides were drastically lower than predicted, we suggest that the labeled and unlabeled peptides chromatographed differently by HPLC, as expected by the introduction of a hydrophobic photophore as well as differences in charge contributed by the three negatively-charged phosphates in the photolabel.

The [^{3}H]BZDC-IP$_3$ photoaffinity ligand also selectively labels the IP$_3$R with a 50–60% incorporation efficiency. The higher efficiency rates of incorporation of the benzophenone-type photoaffinity moiety make this class of ligands ideal for sequencing of photolabeled peptides where higher labeling efficiencies and purification yields are required. Benzophenone-derived photoaffinity ligands, based on incorporating the *p*-benzoylphenylalanine unit into polypeptide ligands, have only recently been employed for labeling peptides within receptor or enzyme proteins (Kauer et al., 1986; Miller & Kaiser, 1988; Boyd et al., 1991). Miller and Kaiser (1988) successfully sequenced a peptide fragment from within the cAMP-dependent protein kinase substrate binding domain

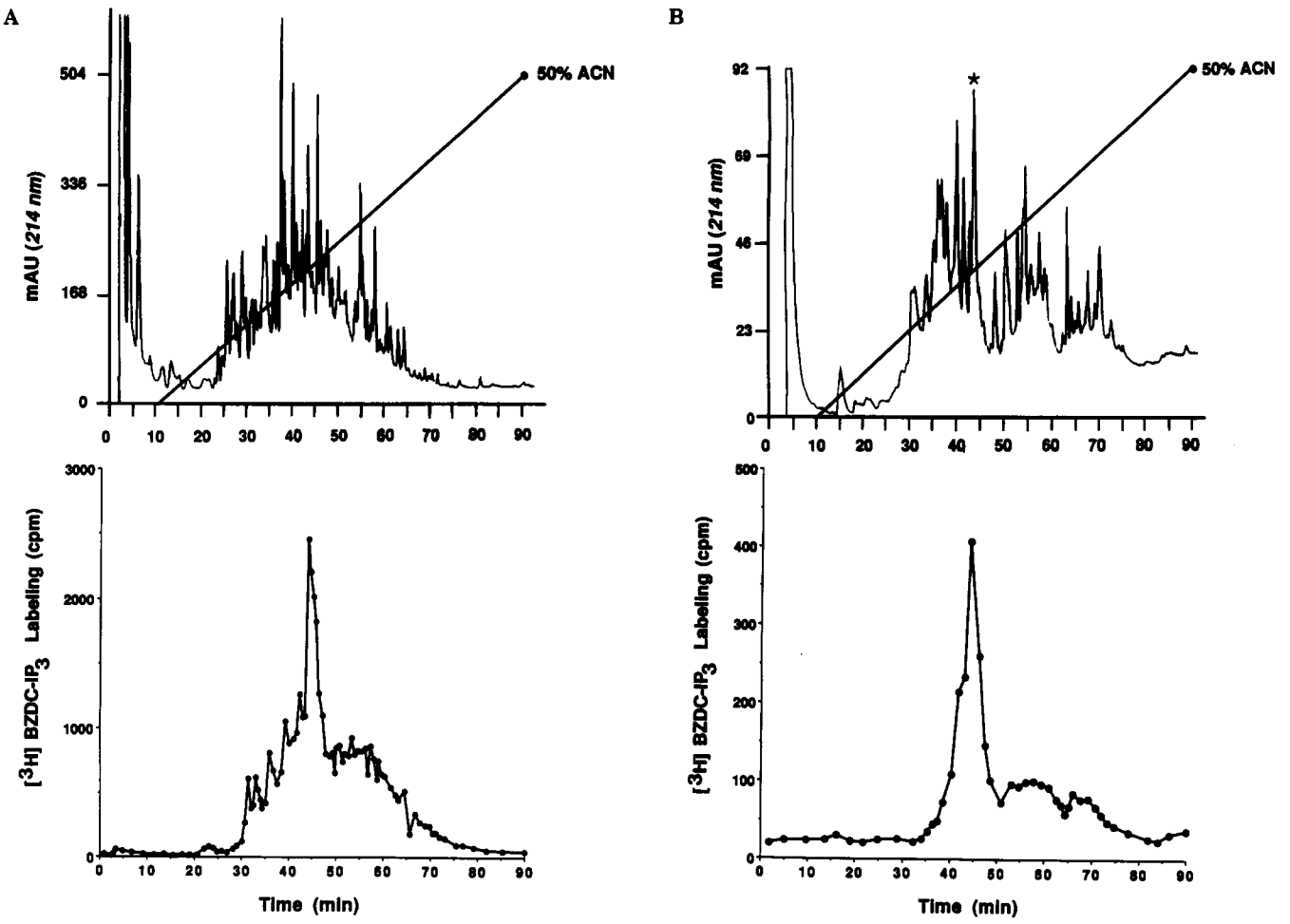

FIGURE 7: Purification of [^{3}H]BZDC-IP_3-labeled peptides. Peptides were purified using (A) C_8 reverse-phase and (B) phenyl reverse-phase HPLC chromatography as described in Materials and Methods using a linear 0–50% acetonitrile gradient from 10 to 90 min. Upper traces represent monitoring of peptides by absorbance, and lower traces represent radioactivity assayed in 20 μL from each peak fraction. Trypsin digests were split into four 200-μL fractions for injection onto the C_8 column. Panel A shows a representative trace of nearly four identical runs. The radioactive peak, fractions 40–50 min, from each run were combined, concentrated, and injected onto the phenyl column. The asterisk in panel B denotes the purified radiolabeled peptide that was sequenced (peptide 1).

labeled with a benzophenone photoaffinity ligand. However, this present work described the first nonpeptide ligand and the first use of the *p*-benzoylcinnamide group as a photophore. This novel photolabel, which is both photolabile and tritiated, offers new opportunities for peptide mapping via photoaffinity labeling.

The peptide we sequenced lies in the N-terminal 20% of IP_3R, fitting with predictions for the location of the IP_3 binding site estimated by deletion mutagenesis. Miyawaki et al. (1991) constructed mutants with 22 selected deletions. IP_3 binding was systematically lost with four mutants that contain three separate deletions and one overlapping segment of deletions in the extreme N-terminal portion of the receptor. Our peptide sequence overlaps the region deleted from the mutant lacking amino acids 419–735 and lies adjacent to a second mutant with positions 169–465 deleted. The photolabeled peptide does not fall within Miyawaki's third (aa 96–315) and fourth (aa 316–352) IP_3 binding mutant. This discrepancy may be explained by conformational changes induced by deleting those amino acid regions that prevent IP_3 binding. Alternatively, a second peptide region may be involved in IP_3 binding that we were unable to photolabel in sufficient quantities to purify and sequence. The amino acid sequence of the photolabeled tryptic IP_3R peptide contains an overall acidic charge with a predicted isoelectric point of 3.6. This region of the IP_3R also generates acidic peptides upon proteolysis by thermolysin, CNBr, and endoproteinase Glu-C. The amino acid content in this IP_3R region may explain the acidic migration observed with photolabeled IP_3R peptides in Figure 6.

The coincidence of the deletion data with the peptide labeled by our selective IP_3 photoaffinity supports the conclusion that our ligand binds at or very close to the IP_3 recognition site. Because photoaffinity ligands are inherently chemically reactive, they might form covalent linkages with sites other than the specific recognition site on the receptor. In addition, the reactive group is situated some distance from the actual contact points for the three critical charged phosphate groups. Nonetheless, considerable specificity of the photoaffinity ligand binding to IP_3R strongly suggests that covalent binding occurs at the physiologic IP_3 recognition site.

Photoaffinity ligands have been employed extensively to label proteins. Their successful use to obtain the amino acid sequence of sites on proteins that bind ligands, however, is limited (Carlstedt-Duke et al., 1988; Dennis et al., 1988; Stephenson & Duggan 1989; Greenberger et al., 1991; Nakayama et al., 1991; Middleton & Cohen, 1991; Yip et al., 1991). The direct sequencing of photolabeled peptides to determine the ligand binding site of a physiological receptor is even more rare, having been accomplished with the nicotinic acetylcholine receptor (Dennis et al., 1988; Middleton & Cohen, 1991). Difficulties include the complexities involved in purifying labeled peptides from a mixture of large numbers of peptides derived from receptor proteins that typically are of high molecular weight. The IP_3R is evidently the largest

Table II: Amino Acid Sequence of a Purified [^{3}H]BZDC-IP$_3$-Photolabeled Peptide[a]

cycle no.	AA	pmol	rat IP$_3$R
1	L	151	L (476)
2	L	140	L
3	E	89	E
4	D	51	D
5	L	39	L
6	V	14	V
7	X		Y
8			F
9			V
10			T
11			G
12			G
14			N
15			S
16			G
17			Q
18			D
19			V
20			L
21			E
22			V
23			V
24			F
25			S
26			K (501)

[a] [^{3}H]BZDC-IP$_3$-photolabeled peptides were prepared and purified as described in Materials and Methods. Peptide 1 was purified and sequenced twice with the same results. Rat IP$_3$ receptor sequences were taken from published data (Mignery et al., 1990), and numbers in parentheses correspond to amino acid numbers from these sequences. AA = amino acid; X = sequencing reaction stopped.

receptor protein for which a ligand recognition site has been directly sequenced.

ACKNOWLEDGMENT

We thank C. D. Ferris and A. B. Theibert for helpful discussions, Wu-Schyong Liu for expert assistance in sequencing the peptides, and Dr. David G. Ahern (DuPont/NEN) for tritium labeling.

REFERENCES

Berridge, M. J., & Irvine, R. F. (1989) *Nature 341*, 197–204.
Boyd, N. D., White, C. F., Cerpa, R., Kaiser, E. T., & Leeman, S. E. (1991) *Biochemistry 30*, 336–342.
Carlstedt-Duke, J., Stromstedt, P. E., Persson, B., Cederlund, E., Gustafsson, J. A., & Jornvall, H. (1988) *J. Biol. Chem. 263*, 6842–6846.
Chuang, D. M. (1989) *Annu. Rev. Pharmacol. Toxicol. 29*, 71–110.
Danoff, S. K., Ferris, C. D., Donath, C., Fischer, G., Munemitsu, S., Ullrich, A., Snyder, S. H., & Ross, C. A. (1991) *Proc. Acad. Natl. Sci. U.S.A. 88*, 2951–2955.
Dennis, M., Giraudat, J., Kotzyba-Hibert, F., Goeldner, M., Hirth, C., Chang, J., Lazure, C., Chretien, M., & Changeux, J. P. (1988) *Biochemistry 27*, 2346–2357.
Ferris, C. D., & Snyder, S. H. (1992) *Annu. Rev. Physiol. 54*, 469–488.
Ferris, C. D., Huganir, R. L., Supattapone, S., & Snyder, S. H. (1990) *Nature 342*, 87–89.
Ferris, C. D., Cameron, A. M., Bredt, D. S., Huganir, R. L., & Snyder, S. H. (1991) *Biochem. Biophys. Res. Commun. 175*, 192–198.
Fischer, S. K., Heacock, A. M., & Agranoff, B. W. (1992) *J. Neurochem. 58*, 18–38.
Furuichi, T., Yoshikawa, S., Miyawaki, A., Wada, K., Maeda, N., & Mikoshiba, K. (1989) *Nature 342*, 32–38.
Greenberger, L. M., Lisanti, C. J., Silva, J. T., & Horwitz, S. B. (1991) *J. Biol. Chem. 266*, 20744–20751.
Huganir, R. L., Miles, K., & Greengard, P. (1984) *Proc. Natl. Acad. Sci. U.S.A. 81*, 6968–6872.
Ji, I., Shin, J., & Ji, T. H. (1985) *Anal. Biochem. 151*, 348–349.
Kalinoski, D. L., Aldinger, S. B., Boyle, A. G., Hugue, T., Marecek, J. F., Prestwich, G. D., & Restrepo, D. (1992) *Biochem. J. 281*, 449–456.
Kauer, J. C., Erickson-Viitanen, S., Wolfe, H. R., Jr., & DeGrado, W. F. (1986) *J. Biol. Chem. 261*, 10695–10700.
Kuno, M., & Gardner, P. (1987) *Nature 326*, 301–304.
Laemmli, U. K. (1970) *Nature 227*, 680–685.
Leyva, E., Munoz, D., & Platz, M. S. (1989) *J. Org. Chem. 54*, 5938–5945.
Middleton, R. E., & Cohen, J. B. (1991) *Biochemistry 30*, 6987–6997.
Mignery, G. A., & Südhof, T. C. (1990) *EMBO J. 9*, 3893–3898.
Mignery, G. A., Newton, C. L., Archer, B. T., III, & Südhof, T. C. (1990) *J. Biol. Chem. 265*, 12679–12685.
Miller, W. T., & Kaiser, E. T. (1988) *Proc. Natl. Acad. Sci. U.S.A. 85*, 5429–5433.
Miyawaki, A., Furuichi, T., Ryou, Y., Yoshikawa, S., Nakagawa, T., Saitoh, T., & Mikoshiba, K. (1991) *Proc. Natl. Acad. Sci. U.S.A. 88*, 4911–4915.
Mourey, R. J., Verma, A., Supattapone, S., & Snyder, S. H. (1990) *Biochem. J. 272*, 383–389.
Nakagawa, T., Okano, H., Furuichi, T., Aruga, J., & Mikoshiba, K. (1991) *Proc. Natl. Acad. Sci. U.S.A. 88*, 6244–6248.
Nakayama, H., Taki, M., Striessnig, J., Glossmann, H., Catterall, W. A., & Kanaoka, Y. (1991) *Proc. Natl. Acad. Sci. U.S.A. 88*, 9203–9207.
Otsu, H., Yamamoto, A., Maeda, N., Mikoshiba, K., & Tashiro, Y. (1990) *Cell Struct. Funct. 15*, 163–173.
Prestwich, G. D., Marecek, J. F., Mourey, R. J., Theibert, A. B., Ferris, C. D., Danoff, S. K., & Snyder, S. H. (1991) *J. Am. Chem. Soc. 113*, 1822–1825.
Ronnett, G. V., & Snyder, S. H. (1992) *Trends Neurosci.* (in press).
Ross, C. A., Meldolesi, J., Milner, T. A., Satoh, T., Supattapone, S., & Snyder, S. H. (1989) *Nature 339*, 468–470.
Ross, C. A., Danoff, S. K., Ferris, C. D., Donath, C., Fischer, G. A., Munemitsu, S., Snyder, S. H., and Ullrich, A. (1991) *Neurosci. Abstr. 17*, 18.
Satoh, T., Ross, C. A., Villa, A., Supattapone, S., Pozzan, T., Snyder, S. H., & Meldolesi, J. (1990) *J. Cell Biol. 111*, 615–624.
Schäfer, R., Nehls-Sahabandu, M., Brabowsky, B., Dehlinger-Kremer, M., Schultz, I., & Mayr, G. W. (1990) *Biochem. J. 272*, 817–825.
Stephenson, F. A., & Duggan, M. J. (1989) *Biochem. J. 264*, 199–206.
Supattapone, S., Worley, P. F., Baraban, J. M., & Snyder, S. H. (1988) *J. Biol. Chem. 263*, 1530–1534.
Theibert, A. B., Estevez, V. A., Mourey, R. J., Marecek, J. M., Barrow, R. K., Prestwich, G. D., & Snyder, S. H. (1992) *J. Biol. Chem. 267*, 9071–9079.
Watt, D. S., Kawada, K., Leyva, E., & Platz, M. S. (1989) *Tetrahedron Lett. 30*, 899–902.
Yip, C. C., Grunfeld, C., & Goldfine, I. D. (1991) *Biochem. 30*, 695–701.